

CRITICAL ANALYSIS OF "MAXIMUM STRESS FAILURE CRITERION" FOR COMPOSITE MATERIALS

Ion FUIOREA, Dumitrița STĂNICĂ

Calculation and Testing Institute for Aero-Astronautics Structures, București
email: ifuiorea@straero.ro

ABSTRACT

The paper deals with critical considerations upon different points of view that were enounced by some authors referring to Maximum Stress Failure Criterion for composite materials. The considerations stem both from a comparative analysis of the mentioned theories and from the results of theoretical and numerical tests performed by the authors.

KEYWORDS: failure criterion, composite materials

1. Introduction

One of the most important phase of the structure design consists in the evaluation of the structure load-carrying capacity. The appreciation of the failure moment depends on the contribution of each component of stress tensor to the failure process in each point where analysis was performed.

In the special case of composites, the problem becomes more complicated as a result of the mixture of different materials with obvious different mechanical properties (inclusively strengths). If a failure criterion was defined, the problem of load-carrying capacity stems from the evaluation of the position with respect to value 1 of the mathematic expression of the criterion

$$F(\sigma_1, \sigma_2, \tau_{12}) <, =, > 1. \quad (1)$$

In the space of stresses $\sigma_1, \sigma_2, \tau_{12}$, (1) describes a so-called failure surface that is represented in fig. 1.

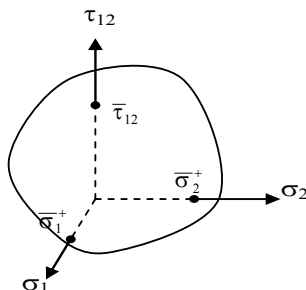


Fig. 1. Failure surface for plane stress state

Unlike the isotropic case, in (1) the coefficients represent the anisotropy principal directions for plane stress state.

The most used failure criterions are as follows:

- Maximum Stress Failure Criterion;
- Maximum Strain Failure Criterion;
- Hill-Mises Criterion;
- Tsai-Hill Criterion;
- Tsai-Wu Criterion;
- Fracture Mode Criterion;
- Hoffman Criterion;
- Quadratic Criterion;
- Interactive Fracture Criterion.

Despite its major inconvenient, the *Maximum Stress Failure Criterion* is sometimes used to design composite structures because it is simple and conservative, i.e., it underestimates material strength increasing the safety factor for the structure under design.

2. Brief description of the criterion

This criterion belongs to a structural type and is based on the assumption that there can exist three possible modes of failure caused by stresses $\sigma_1, \sigma_2, \tau_{12}$, when one of them reaches the corresponding ultimate value; or, mathematically

$$\begin{aligned} \sigma_1 \leq \bar{\sigma}_1^+, \quad \sigma_2 \leq \bar{\sigma}_2^+, \quad \text{if } \sigma_1 > 0, \quad \sigma_2 > 0, \\ |\sigma_1| \leq \bar{\sigma}_1^-, \quad |\sigma_2| \leq \bar{\sigma}_2^-, \quad \text{if } \sigma_1 < 0, \quad \sigma_2 < 0, \\ |\tau_{12}| \leq \bar{\tau}_{12} \end{aligned} \quad (2)$$

NB. In (2) all values for ultimate stresses $\bar{\sigma}^+$ for tensile strength, $\bar{\sigma}^-$ for compressive strength and $\bar{\tau}$ for shearing strength are taken as positive quantities.

As it can be seen, in this criterion the failure is associated with independently acting stresses and the possible stress interaction is ignored. According to the equations (2) the failure surface described in fig. 1 becomes as shown in fig. 2.

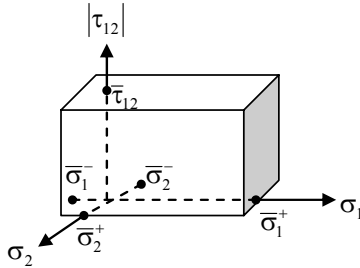


Fig. 2. Failure surface for maximum stress criterion

A simple analysis of the criterion can lead to the main applicability cases: generally for simple structural elements where a certain loading scheme induces one of the three components of stresses $\sigma_1, \sigma_2, \tau_{12}$, obviously greater than the other two. As an example a turbine compressor blade is loaded especially along its own axes by centrifugal forces, developing an axial prevailing stress (fig. 3).



Fig. 3. Prevailing uniaxial stress loading

3. Physical experiments

A number of physical tests were performed in order to verify the accuracy of the criterion prescriptions. Because simple uniaxial tests can lead only to the intersection points of the axes with the failure surface (fig. 2), complex loading schemes were considered. For graphical representation reasons the loading schemes were in one of the planes (σ_1, σ_2) , (σ_1, τ_{12}) or (σ_2, τ_{12}) referring to the notations in fig. 2.

3.1. Tensile-compression experiments in (σ_1, σ_2) plane

A set of complex failure experiments was performed by G. Prokhorov and N. Volkov upon a glass-epoxy fabric composite [1]. The tests were performed by using a biaxial testing machine, one direction in tensile and the other in tensile and

compression senses of loading. The results were briefly presented in figure 4.

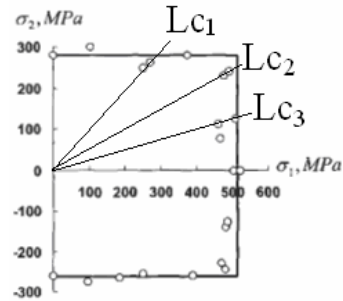


Fig. 4. Tensile-compression failure envelope for glass-epoxy fabric composite

Some remarks can be made analyzing the graphics in fig. 4:

- all experiments denote that failure curve overestimates the material strength;
- the maximum error of the criterion predictions is about 9%;
- each loading case (LC_i) was considered for a certain σ_1/σ_2 ratio;
- two experiments were performed for each load case resulting in an average spread of about 4.3%.

3.2. Experiments in (σ_1, τ_{12}) plane

Annin and Baev [1] studied the same criterion performing complex failure experiments considering tensile and shearing loading upon a glass-epoxy fabric composite. The tests were performed by using cylindrical samples (considering torsion simultaneously applying together with tensile loading). The results were briefly presented in figure 5.

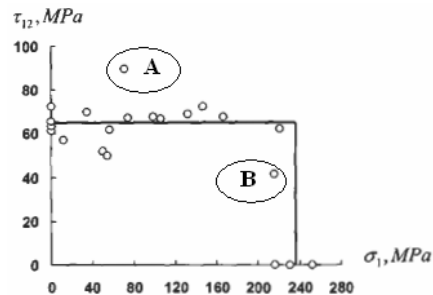


Fig. 5. Tensile-shearing failure envelope for glass-epoxy fabric composite

Some remarks can be made analyzing the graphics in fig. 5:

- eliminating the A & B experiments it can be considered that the criterion provides a satisfactory prediction of strength;
- the maximum error of the criterion predictions is about 12%;

- a certain loading case was not repeated and, in consequence no conclusion regarding the average result spread can be considered.

3.3. Biaxial compression experiments in (σ_1, σ_2) plane

As it was already highlighted, this criterion ignores the interaction of stresses during the damage process. The previous types of tests offered results considered satisfactory enough.

However some tests upon composites on cross samples which were loaded with compression in two orthogonal directions denoted strong interaction of the stresses. As an example in fig. 6 we represented the corresponding experimental results from Belyankin et al.

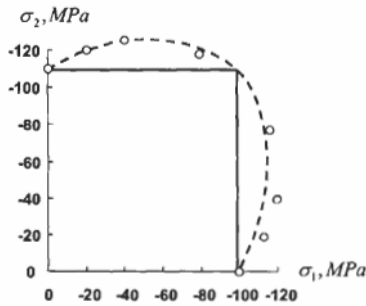


Fig. 6. Biaxial compression failure envelope for glass-phenolic fabric composite

Analyzing the diagram in fig. 6, some remarks can be considered:

- a considerable deviation of the experimental data from the prescriptions of the criterion can be noticed;
- a maximum deviation of the experimental data exceeds 20% (22.31%);
- another criterion that takes into account the mutual influence of the simultaneous stresses seems to fit better; (as an example in fig. 6 the prescriptions of the polynomial-tensorial criterion was drawn in dotted line).

V Vasiliev and E Morozov in [1] offer an interesting explanation of this behavior of composite: "compression of the filling yarns increases the strength in the wrap direction and vice versa".

Another explanation of the phenomenon that can be considered for isotropic materials too, in this case of loading, can be: *the compression on one direction produces, in normal cases, transversal dilatation on the orthogonal direction but this is blocked by the compressive loading on that direction. As a consequence, this tendency of dilatation can be translated as forces that reduce the intensity of the applied ones and the increase of the material strength.*

Mathematically this explanation can be quantified considering the loading case with respect to fig. 7.

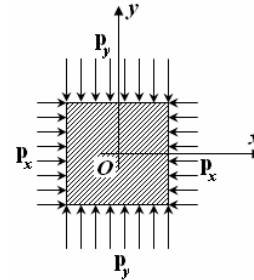


Fig. 7. Biaxial compression scheme

If only p_x is acting, it produces a dilatation of the specimen towards Oy axis given by

$$\varepsilon_y = -\frac{\nu_{xy}}{E_x} \cdot p_x \quad (3)$$

In order to vanish this deformation, a p_y pressure given by

$$p_y = \frac{E_y}{E_x} \cdot \nu_{xy} \cdot p_x \quad (4)$$

will be necessary. That means that only a pressure given by

$$p_{yef} = p_y - \frac{E_y}{E_x} \cdot \nu_{xy} \cdot p_x \quad (5)$$

will effectively produce compression towards Oy axis.

In a similar way, the effective compressing pressure on Ox axis will be

$$p_{xef} = p_x - \frac{E_x}{E_y} \cdot \nu_{yx} \cdot p_y \quad (6)$$

The considerations previously mentioned can be accepted only if Ox and Oy are the principal axis of anisotropy, respectively, the direction of fibers (filling yarn direction and wrap direction). If other directions are considered the coupling effects have to be considered and shearing deformations will appear.

The main consequence of blocking the transversal contraction on Ox and Oy direction is a cumulative effect of dilatation towards Oz axis given by

$$\varepsilon_z = -\frac{\nu_{xz}}{E_x} \cdot p_x - \frac{\nu_{yz}}{E_y} \cdot p_y \quad (7)$$

A general conclusion that can be considered in this case is that the maximum strength failure criterion underestimates the strength and, accordingly, it increases substantially the real safety factor for composites structures. The increasing of safety factor constitutes an undesirable effect for composite aircraft structures where the factor is imposed by regulations around 1.5. (Higher values of the factor will increase the weight of the structure).

4. Numerical off-axis tensile experiments

The simplest way to induce a complex plane stress state is to perform off-axis tensile experiments. As in the previous cases the main problem was to realize the identical manufactured type of composite to ensure a correct comparison of the results.

4.1. Type of considered specimens

The samples can be manufactured either as plane specimens cut from the same panel on different directions, or as cylindrical specimens identically manufactured. As the second way needs special manufacturing technologies (in order to assure identical microstructures with identical macromechanical characteristics) the authors preferred the first type of specimens.

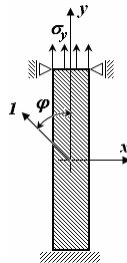


Fig. 7. Type of considered specimen and boundary condition model

Applying stress σ_y as in fig. 7, σ_1 , σ_2 and τ_{12} stresses will be obtained in each point of the specimen. Considering the notations used in eq. (2) and noting $\bar{\sigma}_y$ the ultimate stress on y direction as well, the equations (2) become

$$\bar{\sigma}_y = \frac{\bar{\sigma}_1^+}{\cos^2 \varphi}, \bar{\sigma}_y = \frac{\bar{\sigma}_2^+}{\sin^2 \varphi}, \bar{\sigma}_y = \frac{\bar{\tau}_{12}^+}{\sin \varphi \cos \varphi}. \quad (7)$$

Obviously, the ultimate stress will consider the minimum value obtained from the three equations given by (7).

4.2. Numerical experiments

Some numerical experiments were considered in order to anticipate the physical experimental results.

4.2.1. Specimen model

Considering that the global failure of the specimen is a result of the failure of either fibers or matrix, a micromechanical model of lamina was considered, renouncing at the macromechanical one (homogenous and anisotropic) generally recommended in the literature.

A glass-epoxy composite with $v = 0.5$ volume fraction was considered.

Because the ratio of real diameter of the fibers (aprox. $8\mu\text{m}$) with respect to the specimen dimensions (ρ) will induce an enormous number of equations, a

study of the influence of the ratio on the results was done.

The comparative term for the analysis was considered the equivalent stress in the middle of the specimen, and an error of 10^{-3} was considered satisfactory.

A ratio $\rho = 3 \cdot 10^{-4}$ was considered satisfactory for the purpose of the study.

4.2.1.1. Mathematical model of materials

A linear elastic model was considered both for fibers and for matrix with the principal mechanical characteristics [2]:

Table 1. Mechanical characteristics

Material/Characteristics	Glass	Epoxy
Tensile strength [MPa]	3200	130
Shearing strength [MPa]	2240	58
Young modulus [MPa]	8.6E4	4.5E3
Poisson ratio	0.2	0.4

4.2.1.2. Finite element model

The numerical simulation was performed considering ANSYS 11 code.

A plane isoparametric triangular element PLANE42 with three degrees of freedom was considered both for fibers and matrix, as well as the following hypothesis:

- the specimen works in a plane stress state;
- the connection between fibers and matrix is perfect (simulated by merging the nodes);
- classical mounting clamps of the testing machine is considered.

In fig. 8 is presented the FEM model of the specimen.

It can be observed that in the plane stress problem the cylindrical shape of the fibers was ignored as well as the possible nonuniform distribution inside matrix.

The orientation of fibers was considered for the study in an automatic way in steps of 5 degrees each.

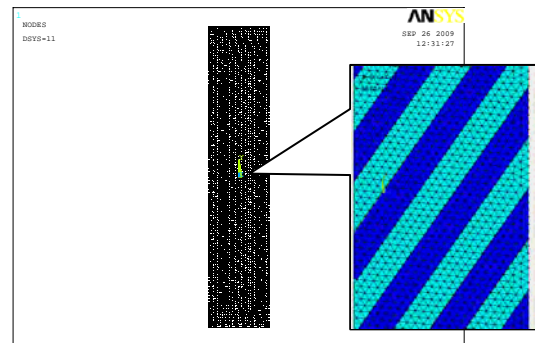


Fig. 8. FEM model of specimen

4.2.1.3. Boundary conditions

As it can easily be noticed from fig. 7, the chosen boundary conditions try to approximate the real loading scheme of the clamps of the testing machine.

4.2.2. Calculus particularities

The calculations were repeated increasing or decreasing the σ_y values until one of the stress components of matrix or fibers reached the ultimate value. The corresponding $\bar{\sigma}_y$ value was noted as the ultimate strength of the lamina.

The parasite theoretical stress concentrations were eliminated.

A direct influence of the width of the specimen upon the calculated results was noticed. In order to eliminate this inconvenient some tests for different values of width were performed to establish the desirable value where the results are not strongly influenced.

For the gamma of the experiments a ratio of 1/14.5 was considered acceptable. As a result of tests (considering the equivalent stress in the middle of the specimen) it resulted that the desirable width of the specimen for a certain direction of fibers must ensure the continuity of a part of fibers between the clamps of the machine.

Theoretically an infinite width of the specimen would be optimum.

The direct conclusion is that the cylindrical specimens eliminate totally this inconvenient and would ensure more accurate results.

4.3. Numerical results

In fig. 9 an example of stress map is presented for the angle of fibers of 35° when the failure of the specimen took place as a result of shearing of the resin along the fibers.

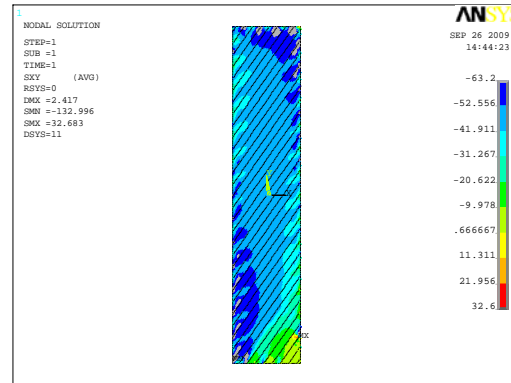


Fig. 9. Stress map for 35° fiber orientation

A simple analysis of the map denotes that the interruption of the fibers between the clamps leads to boundary effects, and sustains the cylindrical specimen shape.

In the table 2, there are presented the resulted ultimate strength of the specimen that was obtained for different orientations of fibers. At the same time, in the table, we presented the modes of the damage that generates the failure of the specimen too: fracture of fibers, fracture inside matrix, shearing of the matrix along the fibers.

Table 2. Numerical results

φ	$\bar{\sigma}_y$	$\frac{\bar{\sigma}_1^+}{\cos^2 \varphi}$	$\frac{\bar{\sigma}_2^+}{\sin^2 \varphi}$	$\frac{\bar{\tau}_{12}^+}{\sin \varphi \cos \varphi}$	φ	$\bar{\sigma}_y$	$\frac{\bar{\sigma}_1^+}{\cos^2 \varphi}$	$\frac{\bar{\sigma}_2^+}{\sin^2 \varphi}$	$\frac{\bar{\tau}_{12}^+}{\sin \varphi \cos \varphi}$
[Deg]	[MPa]				[Deg]	[MPa]			
0	1667	1667			50	119.02		221.5927	127.9363
5	673	1679.755			55	120.11		193.7869	134.0687
10	343	1718.809		368.466	60	121		173.3729	145.4591
15	229			252.0431	65	122.3		158.2992	164.4223
20	177.75			196.052	70	124		147.2464	195.9136
25	149.25			164.504	75	126.12		139.352	
30	134.5			145.5089	80	128.02		134.0549	
35	124.5			134.0977	85	129.1		131.0015	
40	118.5			127.9497	90	130.02		130	
45	117.1		260.0771	126					

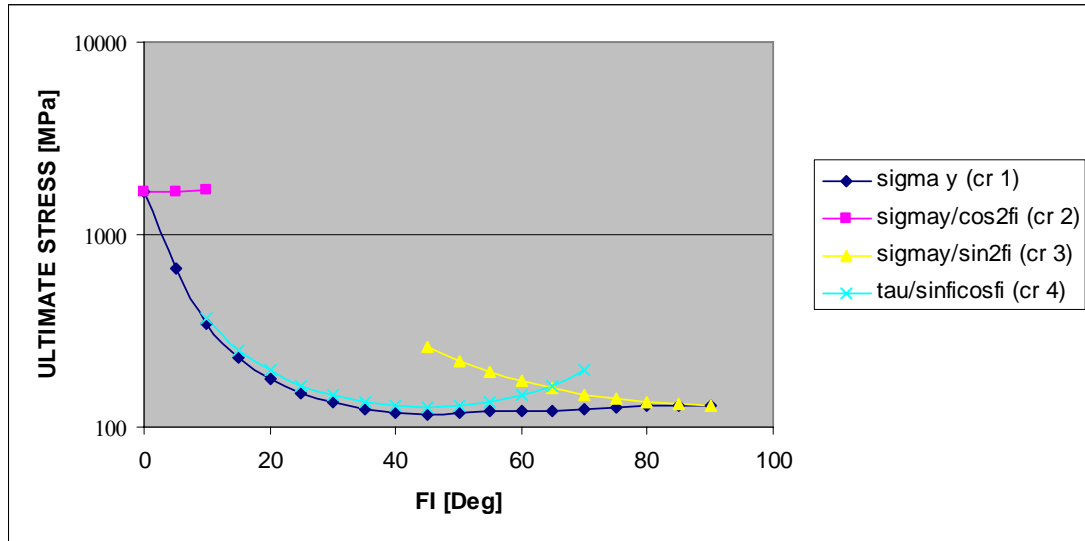


Fig. 10. Ultimate stress variation with respect to fibers orientation

As the legend indicates in fig. 10:

- curve 1 represents the variation of the ultimate strain of the lamina with respect to fibers orientation as a result of numerical tests;
- curve 2 represents the variation of the ultimate strain of the lamina with respect to fibers orientation according to first eq. in (7);
- curve 3 represents the variation of the ultimate strain of the lamina with respect to fibers orientation according to second eq. in (7);
- curve 4 represents the variation of the ultimate strain of the lamina with respect to fibers orientation according to third eq. in (7).

Analyzing the fracture mode of the specimen with respect to the fiber orientation from eq. (7) as well as from the numerical results given in table 2 and synthesized in the graphic from fig. 10, some observation can be done:

- for $\varphi = 0^\circ$ the failure takes place as a result of fiber damage;
- for $5^\circ < \varphi < 65^\circ$ the failure takes place as a result of matrix damage because of shearing ultimate stress;
- for $65^\circ < \varphi < 90^\circ$ the failure takes place as a result of matrix damage because of equivalent ultimate stress.

NB. If the eq.

$$\sigma_y = \frac{\bar{\sigma}_2^+}{\sin^2 \varphi} = \frac{\bar{\tau}_{12}^+}{\sin \varphi \cos \varphi}, \quad (8)$$

will be solved for a certain type of composite the point of separation between matrix shearing failure zone and matrix tensile failure can be found. For the case under analysis the solution of equation (8) was found $\varphi = 66,4^\circ$ and this satisfactorily resulted from numerical tests, $\varphi = 65^\circ$.

- The minimum value of ultimate strength is not for $\varphi = 90^\circ$; For the particular studied case $\bar{\sigma}_{ymin} = 117.1 \text{ MPa}$ and it corresponds for a direction of fibers of about 45° . The direction of fibers for the minimum value of ultimate strength depends on the value of the ratio of matrix ultimate shear strength and matrix ultimate tensile strength.

N.B. For theoretical cases governed by eq. (7) the minimum value for ultimate strength in the availability domain of the third relation, will be obtained solving the eq.

$$\frac{\partial \bar{\sigma}_y}{\partial \varphi} = \frac{\partial}{\partial \varphi} \left(\frac{\bar{\tau}_{12}^+}{\sin \varphi \cos \varphi} \right) = 0. \quad (9)$$

The resulted solution of the eq. (9) is

$$\varphi = \pm 45^\circ. \quad (10)$$

A very good concordance with the numerical experiment can be noticed too.

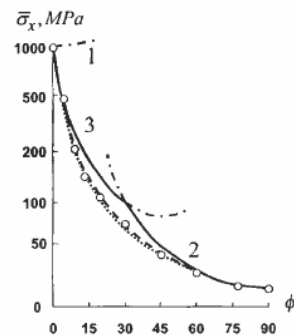


Fig. 11. Jones ultimate tensile experiments, 1, 2, 3 curves corresponding to eq. (7) and "o" experimental tensile data.



As a supplementary validation of the numerical experiments, some experimental data taken from Jones [3] will be considered. A quite good concordance of the experimental data with the numerical ones denotes satisfactory results able to validate the numerical model.

Because of the mechanical characteristics of the composite tested by Jones (matrix shearing ultimate stress much inferior to the tensile one) the intersection point of (2) and (3) curves is strongly deviated to the left (30°).

As a general validation, the modes of failure are similar both in the physical and numerical tests.

5. Conclusions

1. The ultimate strength failure criterion ignores the interaction of stresses and this leads to an underestimation of the failure; as a result, of an increasing safety factor and a corresponding increasing structure weight will be noticed.
2. In some cases, the criterion can be used to design the composite structures, because it is simple and conservative, especially for simple structural elements where a certain loading scheme induces one of the three components of stresses $\sigma_1, \sigma_2, \tau_{12}$, obviously greater than the other two.
3. Numerical tests offer a general spectrum of the failure tests generating enough satisfactory data.
4. Physical failure tests on similar samples as the simulated ones will consist in the next step in the criterion description and analysis.

References

- [1]. Valery V Vasiliev & Evgeny V Morozov - *Mechanics and Analysis of Composite Materials*, Elsevier, 2001, Amsterdam. London. New York. Oxford. Paris. Shannon Tokyo
- [2]. Gay Daniel - *Matériaux composites*, 3^e Édition revue et augmentée, Hermes, Paris, 1990
- [3]. Jones, R.M. - *Mechanics of Composite materials*. 2nd edn. Taylor and Francis, Philadelphia, 1999
- [4]. Fuiorea I. - *Mecanica Materialelor Compozite. Proiectarea Răspunsului Mecanic*. Ed. Pan Publishing House, București, 1998.